Indian Journal of Biochemistry & Biophysics
Vol. 60, March 2023, pp. 167-176
DOI: 10.56042/ijbb.v60i3.66526

miR-145-5p and miR-203a-5p overcome imatinib resistance in myelogenous leukemic cells through metabolic reprogramming

Priyanka Singh[1], Sonu Kumar Gupta[1], Villayat Ali[1], Ravindresh Chhabra[1]* & Malkhey Verma[1,2]*

[1]Department of Biochemistry, School of Basic Sciences, Central University of Punjab, Bathinda-151 401, Punjab, India
[2]School of Biotechnology, Institute of Science, Banaras Hindu University, Varanasi-221 005, Uttar Pradesh, India

Received 14 September 2022; *revised 14 December 2022*

Imatinib is the most effective therapy for chronic myeloid leukemia (CML), but many patients eventually develop resistance to it after an initial satisfactory response. This study investigated the potential of three miRNAs (miR-106b-5p, miR-145-5p, miR-203a-5p) in overcoming imatinib resistance in leukemic cells. The imatinib-resistant K562 (IR-K562) cells were developed and transfected with one of the three miRNAs to evaluate their potency in overcoming imatinib resistance. The changes in the metabolic profile were studied using flux balance analysis (FBA) and the data was validated using qRT-PCR.Among the three miRNAs, the ectopic expression of either miR-145-5p or miR-203a-5p was able to sensitize the IR-K562 cells to imatinib. The concentration of key oncometabolites; glucose, lactate, and glutamine, in the culture media of the miR-transfected IR-K562 cells, reverted to the same levels as seen in imatinib-sensitive K562 cells. In addition, the FBA analysis revealed that the metabolism of lipid, fatty acids, and electron transport chain were significantly altered in resistant cells. The FBA data was also validated at the molecular level. Interestingly, the imatinib treatment coupled with the transfection of miR-145-5p or miR-203a-5p cells could reverse the metabolic flux of IR-K562 to the levels seen in imatinib-sensitive K562 cells. This study highlights the key metabolic changes that occur during development of imatinib resistance. It also identifies the specific miRNAs which can be targeted to overcome imatinib resistance in CML.

Keywords: Chemoresistance, Flux balance analysis (FBA), K562, miRNAs, Oncometabolites

Chronic myeloid leukemia (CML), a myeloproliferative neoplasm, is primarily characterized by the presence of the Philadelphia chromosome. The Philadelphia chromosome has a fusion oncogene called *Breakpoint cluster region-Abelson murine leukemia* (*Bcr-Abl1*), which is formed after *Abl1* region on chromosome 9 is translocated next to *Bcr* region on chromosome 22[1]. The BCR-ABL1 oncoprotein is an "always-on" tyrosine kinase that promotes cell proliferation, cellular adhesion, differentiation, activation of mitogenic signaling, and suppression of apoptosis[2].The first-line treatment for CML has been tried with multiple strategies including tyrosine kinase inhibitors (TKIs), protein translation inhibitors, myelosuppressive medicines, leukapheresis, interferon-alpha, allogeneic stem cell transplantation, and splenectomy. TKIs have, so far, proved to be the most effective as this "targeted" strategy increased the 10-year survival rate from approximately 20% to around 80%-90%[3]. The first TKI breakthrough occurred in the late 1990s when biochemist, Nicholas Linden, at Novartis developed imatinib (Gleevec®), the first synthesized TKI which is still the first choice for CML therapy despite the development of new generation TKIs (dasatinib, nilotinib, bosutinib, ponatinib, and asciminib)[4]. The reason imatinib remains the most preferred therapeutic is that it could offer a satisfactory long-term response in the majority of patients by addressing the 4C issues, *i.e.*, cost, co-morbid conditions, continuous monitoring, and compliance concerns.Imatinib, a 2-phenyl amino pyrimidine derivative, binds to the oncoprotein BCR-ABL1 at the adenosine triphosphate (ATP)-binding site, causing a conformational alteration in the active site motif, Asp-Phe-Gly (DFG) of *ABL1*. This constrains the oncoprotein's kinase activity, and finally suppresses tumorigenesis[5]. Imatinib improves patient survival in the early stages of CML but is not a cure because, at advanced stages of cancer, around 20% of patients acquire resistance to imatinib treatment[6]. Many strategies have been employed to overcome the imatinib resistance in CML but none of them have yielded any significant improvement. In that scenario,

*Correspondence:
Phone: +91-7589489833 (MV); +91-9478723446 (RC) (Mob)
E-mail: malkhey@bhu.ac.in (MV);
ravindresh.chhabra@cup.edu.in (RC)
Suppl. Data available on respective page of NOPR

miRNA-based therapy emerged as a new strategy, because miRNAs can be used as both biomarkers for early tumor diagnosis and an efficient cancer treatment tool[7].

The cell proliferation in CML, like other cancers, is driven by glucose, lactate, and glutamine because they establish a dynamic metabolic landscape for tumorigenesis. Because glucose provides ATP (molecular unit of currency) *via* glycolysis, lactic acid suppresses anticancer immunity, and glutamine donates amino acids, these three are considered the primary "oncometabolites"[8]. Furthermore, the BCR-ABL1 oncoprotein is known to accelerate glucose metabolism by monitoring glycolysis and overexpressing membrane-bound glucose transporters (GLUTs) to mediate glucose absorption[9,10]. Imatinib, on the other hand, inhibits glucose metabolism by facilitating intracellular translocation of GLUTs from the cell surface to the cell interior; however, in resistant cells, the GLUTs remain at the plasma membrane[10,11]. It is clear that glucose and amino acids are required for nucleotide synthesis; and as cancer epitomizes altered nucleotide metabolism, imatinib may limit nucleotide metabolism in the same manner as it inhibited glycometabolism[12]. The current study also evaluated the varying concentrations of these three oncometabolites in the imatinib-sensitive and –resistant cells, as well as the metabolic flux before and after transfection of selected miRNAs in resistant cells. Reaction flux in the current study was quantified through the Recon_2.2 model, which helps to comprehend the complexity of human metabolism by giving an underlying feedback network, *i.e.*, all metabolic processes encoded within the genome[13].

The role of the three miRNAs (miR-106b-5p, miR-145-5p, and miR-203a-5p) was studied in the context of previous findings[14-16], with the hypothesis that these miRNAs would reverse imatinib resistance by regulating the altered level of oncometabolites in resistant leukemic K562 cells. Furthermore, unknown metabolic fluxes were calculated after providing the calculated flux of glucose, lactate, and glutamine from experiments, which aided in assessing the physiological condition of the leukemic cells.

Materials and Methods

Chemicals and databases

Imatinib (Sigma-Aldrich, China), RPMI-1640 cell culture media (HiMedia, India), Fetal bovine serum (Gibco, UK), Trypan Blue (Gibco,USA), EZcount™ MTT Cell Assay kit (HiMedia, India), TRIzol Reagent (Invitrogen, USA), Verso cDNA synthesis kit (ThermoScientific™, Lithuania), KAPA SYBR® FAST qPCR Master Mix (2X) Kit (Sigma-Aldrich, South Africa), miRNAs mimics (miR-106b-5p, miR-145-5p, and miR-203a-5p) (Sigma-Aldrich, USA), Opti-MEM reduced serum medium (Gibco, USA), Lipofectamine™ Transfection Reagent (Invitrogen, USA), Glucose (HiMedia, India), Lactic acid (HiMedia, India), $FeCl_3$ (HiMedia, India),Glutamine and Glutamate Determination Kit (Sigma-Aldrich, USA), MATLAB 8.1 (a computer program that calculates metabolic fluxes) (The Mathworks, Natick, MA), COBRA toolbox (https://opencobra.github.io/cobratoolbox/stable/index.html), Recon_2.2 human model (http://identifiers.org/biomodels.db/MODEL1603150001).

Cell culture

The human CML blast crisis cell line K562 (procured from NCCS Pune, India) was grown in the RPMI-1640 culture medium supplemented with 10% fetal bovine serum (FBS), 100 units 100 units per mL of penicillin, and 100 µg/mL of streptomycin and maintained in a humidified incubator (37˚C, 5% CO_2). After the cells achieved 90% confluency, they were subcultured and seeded at a density of about 1.4×10^5 cells/mL.

Development of imatinib-resistant K562 (IR-K562) cells

Imatinib-resistant K562 (IR-K562) cells were generated by sequential prolonged exposure of K562 cells to escalating imatinib concentrations (10 nM, 25 nM, 50 nM, 75 nM, 100 nM, and 150 nM), and leukemic cells were cultivated for 72 h at each concentration of imatinib. After the establishment of resistant cells, IR-K562 cells were centrifuged, washed with PBS, and were continuously maintained in RPMI-1640 medium supplemented with 100nM imatinib in a humidified incubator (37˚C, 5% CO_2). Consequently, after imatinib treatment, we received two sets of cells: normal/control K562 cells (sensitive to imatinib) (C), and imatinib-resistant K562 (IR-K562/R) cells.

Transfection with miRNA mimics

miRNA mimics (miR-106b-5p, miR-145-5p, andmiR-203a-5p) were selected and transfected in imatinib-resistant K562 (IR-K562/R) using Lipofectamine transfection reagent as per the manufacturer's instructions. The cells were harvested 24 h post-transfection. Four samples thus obtained were: (1) IR-K562 (R), (2) R + miR-106 (IR-K562

cells transfected with miR-106b-5p), (3) R + miR-145 (IR-K562 cells transfected with miR-145-5p), and (4) R + miR-203 (IR-K562 cells transfected with miR-203a-5p).

Cell viability assay

The vitality of the cells was measured using the MTT test following the protocol recommended by the reagent manufacturer. The cells were plated in a 96-well cell culture plate at a density of 0.1×10^5 cells/well with or without imatinib for 24 h. The RPMI-1640 medium was then removed and replaced with fresh media, followed by the MTT assay. The absorbance was taken at 570 nm (measurement wavelength) and 630 nm (reference wavelength) (Spark multimode microplate reader, TECAN). Percent inhibition of proliferation was calculated as a fraction of eitherK562 cells or IR-K562 cells.

Glucose, lactate, and glutamine estimation

The quantification of glucose, lactate, and glutamine in the culture medium collected after centrifugation of different samples (C, R, R + miR-106, R + miR-145, and R + miR-203), all of which had been grown in the collected medium for 24 h, was done using an efficient and inexpensive spectrophotometric method.

For glucose quantification, O-Toluidine (8% *v/v* O-Toluidine reagent made in glacial acetic acid) method was used, and the absorbance of the blue-green colored product was measured at a wavelength of 630 nm. Estimation of lactic acid was done after determination of the absorbance of colored product, formed after the reaction between lactate ions with iron(III) chloride, at 390 nm. Glutamine was determined using Glutamine and Glutamate Determination Kit according to the manufacturer's protocol. The concentration of all three oncometabolite in unknown samples was calculated from their respective standard curves (correlation coefficient, $R^2 \geq 0.95$).

Flux balance analysis

For the flux analysis, the concentrations of glucose, lactate, and glutamine were measured at different time intervals. Then, using the slope of the concentration-time interval graph, the flux of glucose, lactate, and glutamine was calculated. Thereafter, the upper and lower bounds of the corresponding oncometabolites in the model Recon 2.2 were substituted with the calculated experimental fluxes, and the flux distribution across genome-scale metabolism was calculated by constraining the model with experimental fluxes of glucose, lactate, and glutamine *via* MATLAB (Fig. S1).

Real-time PCR

The total RNA was isolated using TRIzol reagent and was reverse transcribed into cDNA by the cDNA synthesis kit according to the manufacturer's protocol. The cDNA synthesis for miRNAs was carried out using miRNA-specific stem-loop primers. After that, the qPCR was performed using SYBR Green qPCR Master Mix kit on StepOne real-time PCR system (Applied Biosystem, California, USA) with specific primers (Table S1). The relative gene quantification was performed in triplicate and expression levels were normalized with GAPDH.

Statistical analysis

All data, expressed as mean ± standard deviation (SD), were analyzed using Prism 6.0 software (GraphPad, San Diego, California). Student's t-tests (paired t-tests) were used to compare two groups of data, and the data was considered statistically significant for $P \leq 0.001$ represented by $^{***,###}$, $P \leq 0.005$ by $^{**,\#\#}$, and $P \leq 0.05$ by $^{*,\#}$.

Results

Development and characterization of imatinib-resistant K562 cells (IR-K562)

Leukemic K562 cells were cultured in gradually increasing doses of imatinib (10, 25, 50, 75, 100, and 150 nM) to develop an IR-K562 cell line. The MTT assay revealed that the cell viability continued to decrease with the increasing concentration till 150 nM (Fig. 1A). The cell viability was 34.4% when the imatinib concentration reached 100 nM in comparison to K562 cells. Further increase in imatinib concentration to 150 nM reduced the cell viability to 25.6%. Since the cell number declined substantially at 150 nM, the viable cells which could withstand the gradual increase in imatinib dosage up to 100 nM were considered IR-K562 cells. This result was similar to earlier publications[17,18]. IR-K562 cells that survived at 100 nM were cultured for three months in RPMI-1640 media containing 100 nM imatinib to enrich resistant cells.

The resistant nature of IR-K562 and the sensitivity of K562 cells to imatinib were confirmed by treating the cells with 100 nM imatinib for 24 h followed by MTT assay (Fig. 1B). When imatinib was supplemented, it was observed that the cell viability of IR-K562 cells and K562 cells was 81.5% and

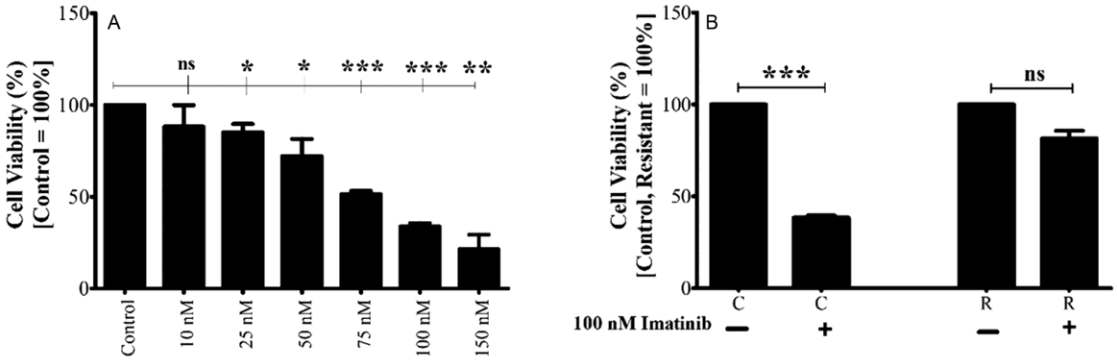

Fig. 1 — MTT assay to determine cell viability (%) (A) Sequential prolonged exposure of imatinib sensitive K562 cells to escalating imatinib concentrations (10, 25, 50, 75, 100, and 150 nM) for 72 h incubation to develop resistant cells (IR-K562); and (B) Untreated K562 cells (control) and IR-K562 cells (resistant) were incubated for 24 h in the absence and presence of 100 nM imatinib to test their resistance to imatinib. *C*: control (normal K562 cells), *R*: imatinib-resistant K562 cells (IR-K562 cells). All data are presented as mean ± SD (n = 3) with statistical significance **P* ≤0.05, ***P* ≤0.005, and ****P* ≤0.0005

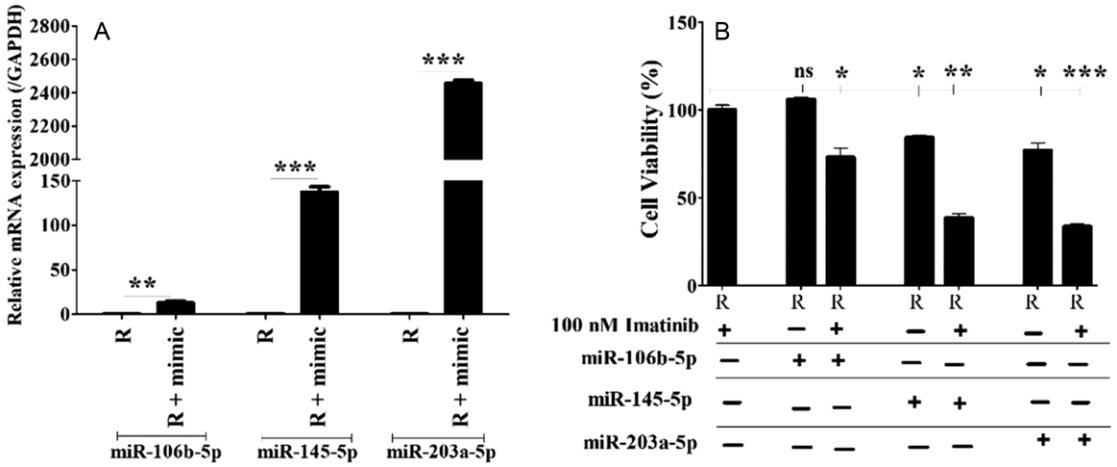

Fig. 2 — (A) Validation of transfection by assessing the relative mRNA expression of miRNAs (miR-106b-5p, miR-145-5p, and miR-203a-5p) (/GAPDH) following transfection; and (B) MTT assay to evaluate cell viability (%) of IR-K562 (R) and miRNAs (miR-106b-5p, miR-145-5p, and miR-203a-5p) transfected IR-K562 (R) cells in the absence and presence of 100 nM imatinib. *R*: imatinib-resistant K562 cells (IR-K562 cells). All data are presented as mean ± SD (n = 3) with statistical significance **P* ≤0.05, ***P* ≤0.005, and ****P* ≤0.0005

38.44% respectively, thus demonstrating that the presence of imatinib does not have a significant effect on *in vitro* developed resistant leukemic cells.

miRNA overexpression overcomes imatinib resistance

MiRNAs are often implicated in cancer chemoresistance[19,20]. miR-106b-5p, miR-145-5p, and miR-203a-5p have been previously shown to be deregulated in imatinib resistance[21-26]. Therefore, we hypothesized that the ectopic expression of these miRNAs may sensitize the resistant cells to imatinib treatment.

The overexpression of the respective miRNAs following their transfection in K562-IR cells was confirmed by qRT-PCR. The expression of miR-106b-5p, miR-145-5p, and miR-203a-5p, increased by about 13, 137, and 2456-fold, respectively, when compared to their endogenous expression in resistant cells (Fig. 2A).

The IR-K562 (R) cells were then subjected to different combinations of imatinib treatment and miRNA overexpression to examine if the imatinib resistance could be overcome with the ectopic expression of miRNAs alone or in conjunction with imatinib. The MTT experiment revealed that imatinib treatment significantly reduced the cell survival of IR-K562 cells whenever a miRNA was over-expressed, except for miR-106b-5p (Fig. 2B). After 24 h of treatment, imatinib + miR-106b-5p, imatinib + miR-145-5p, and imatinib + miR-203a-5p resulted in 73.07%, 38.61%, and 33.64% survival rates,

respectively; whereas treatment of IR-K562(R) cells, only with imatinib, miR-106b-5p, miR-145-5p, and miR-203a-5p, alone resulted in 100%, 100%, 84.34%, and 76.96% cell viability, respectively.

miRNA mediated modulation of oncometabolites (Glucose, Lactate, and Glutamine) in IR-K562 cells

The impact of miRNA overexpression on the Warburg effect in IR-K562 cells was determined through the estimation of glucose, lactate, and glutamine levels. Despite differences in glucose concentrations, the data showed no statistical significance between the glucose level in the culture medium of K562 (549 nmol) and IR-K562 (444 nmol) cells (Fig. 3A). To further evaluate the inhibitory role of miRNAs (miR-106b-5p, miR-145-5p, and miR-203a-5p), glucose level was assessed in transfected resistant cells which was found to be 472 nmol, 492 nmol, and 546 nmol, for miR-106b-5p, miR-145-5p, and miR-203a-5p, respectively. Of the three, the increased glucose in the culture media was statistically significant for miR-145-5p and miR-203a-5p transfected cells, and non-significant for miR-106b-5p when compared with IR-K562 cells (Fig. 3B).

The enhanced production of lactate outside of the cell is often associated with tumorigenesis. It was found that IR-K562 cells (813 µmol) produced significantly higher amounts of lactate in comparison to K562 cells (535 µmol) (Fig. 3B). The lactate production decreased following transfection of any of the three miRNAs, with 754.16 µmol, 598.66 µmol, and 548.64 µmol of lactate in culture media of miR-106b-5p, miR-145-5p, and miR-203a-5p, transfected IR-K562 cells, respectively (Fig. 3B).

The high uptake of glutamine was observed from the culture media of IR-K562 cells (0.260 µmol) compared to K562 cells (0.322 µmol), despite no statistically significant differences between them (Fig. 3C). The glutamine content in the culture medium increased following miRNA transfection in IR-K562 cells to the levels seen in the culture media of K562 cells. Although glutamine consumption was reduced following transfections of miR-106b-5p (0.281 µmol), miR-145-5p (0.313 µmol), and miR-203a-5p (0.332 µmol), compared to resistant cells, there was only median statistical significance in the case of miR-203a-5p and no relevant significance in the case of the other miRNAs (Fig. 3C).

Flux balance analysis reveals miRNA-mediated metabolic changes in resistant K562 cells

The flux of glucose, lactate, and glutamine in distinct groups of cells was calculated; and the influx and efflux values have been symbolized by negative

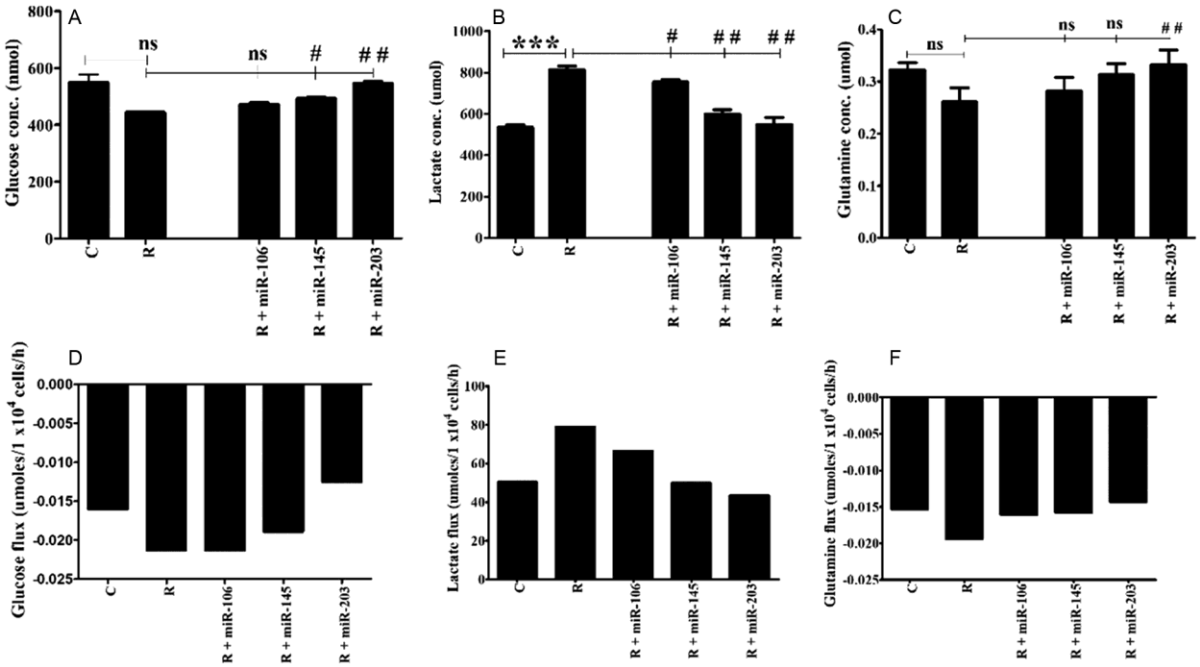

Fig. 3 — (A) Quantification of Glucose level; (B) Quantification of Lactate level; (C) Quantification of Glutamine level; (D) Estimated flux of Glucose; (E) Estimated flux of Lactate; and (F) Estimated flux of Glutamine. *C*: control (normal K562 cells), *R*: imatinib-resistant K562 cells (IR-K562 cells), *R + miR-106*: IR-K562 cells transfected with miR-106b-5p, *R + miR-145*: IR-K562 cells transfected with miR-145-5p, *R + miR-203*: IR-K562 cells transfected with miR-203a-5p. All data are presented as mean ± SD (n = 3) with statistical significance $^{\#}P \leq 0.05$, $^{\#\#}P \leq 0.005$, and $^{\#\#\#}P \leq 0.0005$

and positive integers, respectively. The glucose influx in control cells was −0.016, which increased to -0.0213 in resistant cells; however, after transfection of miRNAs into resistant cells, the flux dropped to -0.0213, -0.0189, and -0.0125 in cells transfected with miR-106b-5p, miR-145-5p, and miR-203a-5p, respectively (Fig. 3D). The lactate efflux for the K562, IR-K562, and miRNAs (miR-106b-5p, miR-145-5p, and miR-203a-5p) transfected cells were determined to be 50.398, 79.064, 66.505, 49.889, and 43.373, respectively (Fig. 3E). The glutamine influx was significantly more in resistant cells (-0.0194) when compared with K562 cells (–0.0153). The glutamine influx reduced when IR-K562 cells were transfected with miR-106b-5p (–0.0161), miR-145-5p (–0.0158), and miR-203a-5p (–0.0143) (Fig. 3F). As expected, the resistant cells showed a higher efflux of lactate and a higher influx of glucose and glutamine than K562 cells, indicating that resistant cells had a higher cell proliferation efficiency. The flux of these oncometabolites in IR-K562 cells, when transfected with miRNAs, reverted to similar levels as were seen for K562 cells. miR-145-5p and miR-203a-5p were considerably more effective.

The human genome-scale metabolic model (Recon 2.2) was constrained with experimental fluxes of glucose, lactate, and glutamine by changing upper and lower bounds; then the flux balance analysis was performed to evaluate the effect before and after transfection. In certain reactions, a large variation in flux values was obtained, whereas, in others, not much change was seen (Table S2). After assessing the flux, it was observed that IR-K562 cells had higher flux values than K562 cells for all reactions, however, the flux was reduced after the IR-K562 cells were transfected with any of the miRNAs (Table S2). The metabolic flux analysis (MFA) demonstrated a remarkable increase in the flux of enzymes involved in carbohydrate, lipid, and fatty acid metabolism, as well as the electron transport chain (ETC) in the IR-K562 cells in comparison to K562 cells (Fig. S2). Interestingly, the ectopic expression of any of the miRNAs (miR-106b-5p, miR-145-5p, and miR-203a-5p) in the resistant cell lines was able to revert the value of these fluxes close to the ones seen in imatinib-sensitive K562 cells (Table 1).

Validation of the MFA analysis at the gene expression level

The MFA analysis was validated at the gene expression level using qRT-PCR. For this, we focussed on the expression analysis of three key enzymes (Aldehyde dehydrogenase, Acetyl-CoA carboxylase, and Acetyl-CoA C-acetyltransferase) that regulate pyruvate consumption in the lipid metabolic process and fatty acid metabolism (Fig. 4A). Aldehyde dehydrogenase (ALDH2) is an important enzyme in metabolic processes that catalyzes the conversion of acetaldehyde to acetate. Acetyl-CoA carboxylase (ACACA) converts acetyl CoA to malonyl CoA, which is subsequently employed in fatty acid synthesis. Apart from its role in fatty acid metabolism, acetyl CoA is also converted from acetate to mevalonate, which is then converted to cholesterol, and lastly to cholesterol ester *via* the enzyme acetyl Co-A C-acetyltransferase (ACAT1). So, by generating cholesterol esters, ACAT1 modulates the lipid metabolic process (Fig. 4A). The gene expression data were concordant with the MFA analysis as it was observed that both miR-145-5p and miR-203a-5p suppressed the expression of all three enzymes in resistant cells.

Table 1 — Flux value of enzymes related to human model Recon_2.2 that regulate different biological processes (influx and efflux values have been symbolized by negative and positive integers, respectively)

S. No.	Enzymes	Control	Resistant	miR-106	miR-145	miR-203
1.	Acetyl-Coa C-Acetyltransferase (ACAT1)	11.85	16.28	14.34	11.77	10.76
2.	Acetyl-Coa Carboxylase (ACACA)	24.51	40.72	33.62	24.22	20.54
3.	Alcohol dehydrogenase (ADH1A)	11.78	16.21	14.27	11.69	10.69
4.	Aldehyde dehydrogenase (ALDH2)	39.16	57.19	49.28	38.83	34.75
5.	Aldose reductase (acetol) (AKR1B1)	11.78	16.21	14.27	11.69	10.69
6.	Alpha-methylacyl-CoA racemase (AMACR)	31.79	48.00	40.90	31.50	27.82
7.	ATP-Citrate Lyase (ACLY)	4.37	9.49	7.25	4.28	3.12
8.	Carnitine O-Aceyltransferase (CRAT)	17.00	26.55	22.36	16.83	14.66
9.	Glucose-6-Phosphate Isomerase (GPI)	-0.16	-0.16	-0.16	-0.16	-0.16
10.	Hydroxymethylglutaryl-Coa Lyase_2 (HMGCLL1)	11.78	16.21	14.27	11.69	10.69
11.	Hydroxysteroid (17-Beta) Dehydrogenase 4 (HSD17B4)	31.79	48.00	40.90	31.50	27.82
12.	Isocitrate Dehydrogenase 2 (IDH2)	-4.37	-9.49	-7.25	-4.28	-3.12
13.	Malic Enzyme (ME1)	4.68	9.80	9.06	3.06	3.42

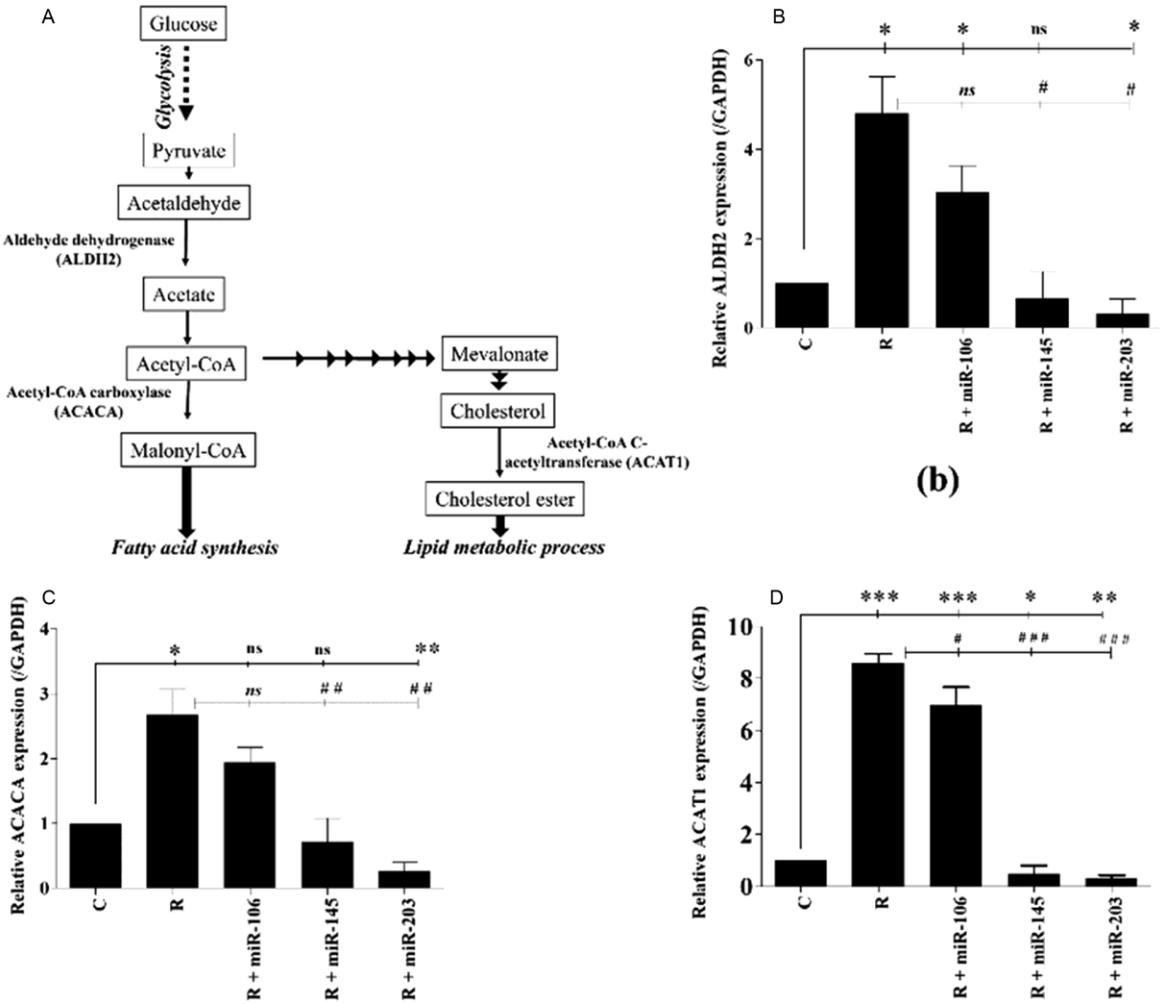

Fig. 4 — (A) Regulation of lipid metabolic process and fatty acid metabolism by Aldehyde dehydrogenase (ALDH2), Acetyl-CoA carboxylase (ACACA), and Acetyl-CoA C-acetyltransferase (ACAT1) (b)Relative mRNA expression of Aldehyde dehydrogenase (ALDH2) (c) Relative mRNA expression of Acetyl-CoA carboxylase (ACACA)(d) Relative mRNA expression of Acetyl-CoA C-acetyltransferase (ACAT1). *C*: control (normal K562 cells), *R*: imatinib-resistant K562 cells (IR-K562 cells), *R + miR-106*: IR-K562 cells transfected with miR-106b-5p, *R + miR-145*: IR-K562 cells transfected with miR-145-5p, and *R + miR-203*: IR-K562 cells transfected with miR-203a-5p. All data are presented as mean ± SD (n = 3) with statistical significance *, $^{\#}P \leq 0.05$, **, $^{\#\#}P \leq 0.005$, and ***, $^{\#\#\#}P \leq 0.0005$

The expression of ALDH2 in IR-K562 was 4.8–fold in comparison with K562 cells (Fig. 4B). The transfection of either miR- 145-5p or miR-203a-5p in IR-K562 cells reduced the expression of ALDH2 by 86% and 93%, respectively in comparison to IR-K562 cells. (Fig. 4B). In the case of ACACA, the expression increased by 2.7–fold in IR-K562 cells when compared with K562 cells. The expression of ACACA was reduced by 73% and 90% following transfection with miR- 145-5p or miR-203a-5p, respectively in comparison to IR-K562 cells (Fig. 4C). Similar data was also obtained with the expression of ACAT1. Its expression increased by 8.6–fold in IR-K562 cells when compared with K562 cells. Following the transfection of miR- 145-5p or miR-203a-5p in IR-K562 cells, the expression of ACAT1 reduced by 94% and 96%, respectively, in comparison to IR-K562 cells (Fig. 4D). miR-106b-5p, however, showed a non-significant effect on ALDH2 and ACACA enzymes and only a slight reduction in the expression of ACAT1 in comparison to IR-K562 cells.

Discussion

The drug, imatinib, has remarkably improved the prognosis of CML patients. Although the majority of CML patients respond well to imatinib treatment, many patients in advanced stages develop resistance.

The possible mechanisms of imatinib resistance could be either due to the mutations in the BCR-ABL1 or the altered cellular metabolisms. The previous reports in the literature implicate miR-106b-5p, miR-145-5p, and miR-203a-5p in cancer chemoresistance[14-17]. Because of this, we investigated these miRNAs to see if they might modify the metabolic profile of resistant leukemic cells and lessen imatinib resistance.

Imatinib-resistant (IR-K562) cells were generated by treating native imatinib-sensitive K562 cells with gradually increasing doses of imatinib.The cells that had grown to be resistant to imatinib were then transfected with miR-106b-5p, miR-145-5p, and miR-203a-5p, of which miR-145-5p and miR-203a-5p effectively overcame resistance. Afterward, the MTT test performed, which revealed that co-administration of imatinib with either miR-145-5p or miR-203a-5p enhanced cell death compared to treatment with imatinib or any miRNA alone. To better understand how oncometabolites contribute to the growth of CML, the current study also measured the levels of glucose, lactate, and glutamine in the different sets of K562 cells. The data in our study showed increased cellular import of glucose and glutamine and increased lactate export in IR-K562 cells when compared with K562 cells. Interestingly, the miR-transfection coupled with imatinib treatment was able to revert the glucose, glutamine, and lactate production in IR-K562 cells, to the levels seen in imatinib-sensitive K562 cells. Among the three miRNAs, miR-145-5p and miR-203a-5p proved to be the most effective. The analysis of metabolic reprogramming was further extended to cover the overall metabolic profile of the imatinib-resistant cell lines using the Flux balance analysis (FBA). FBA assumes that modification in the intracellular metabolite concentrations is induced by flux changes in genes encoding for metabolic enzymes, which then affect various metabolisms, and finally, all of these events together contribute to a pathological condition. In the present study, thirteen enzymes that regulate biological processes (carbohydrate metabolism, lipid metabolism, fatty acid metabolism, ETC) were found to have high influx or outflux values in resistant cells. After overexpressing any of the three miRNAs (miR-106b-5p, miR-145-5p, or miR-203a-5p) in IR-K562 cells, the flux values of these enzymes later returned to the levels seen in K562 cells. The biochemical mechanism underlying imatinib resistance that is miRNA-regulated in K562 cells is highlighted by these data.

The findings of FBA were experimentally validated through qRT-PCR of three key enzymes (ALDH2, ACACA, and ACAT1) involved in the fatty acid synthesis and lipid metabolic pathways. Studies on cancer have demonstrated that downregulation of ALDH2 makes tumor cells more susceptible to anticancer medications. For example, after low expression of ALDH2, bladder cancer cells become sensitive to gentamicin[27], breast and blood cancer cells become sensitive to mitoxantrone[28,29], and clear cell renal cell carcinoma cells become sensitive to anthracycline[30].In this study too, we found that imatinib-resistant cells expressed more ALDH2, which was inhibited by miR-145-5p or miR-203a-5p transfection. ACACA, another fatty acid metabolism key enzyme, has also been studied in imatinib-resistant KU812 CML cells[31]. The expression of this enzyme was also investigated in the current study, and it was discovered that ALDH2 was upregulated in the resistant cells, pointing to a faster rate of lipid synthesis in IR-K562 cells. When miR-145-5p or miR-203a-5p were transfected into IR-K562 cells, this enzyme was, however, downregulated. A third enzyme, ACAT1, which converts cholesterol to cholesterol ester (CE), is gaining popularity in cancer research because it acts as a protumor agent and promotes cell growth[32]. By inhibiting the activity of this enzyme and restoring deregulated cholesterol metabolism, cancers can be treated[33,34]. This assertion is supported by our findings, where ACAT1 expression was high in IR-K562 cells than in control cells and decreased drastically after the transfection of either miR-145-5p or miR-203a-5p.

Conclusion

Imatinib resistance is a major challenge in the treatment of CML patients, and this study highlights a miRNA-based approach to counter imatinib resistance in CML. miR-145-5p and miR-203a-5p were both shown to sensitize resistant cells to imatinib treatment *via* modifying leukemic cell metabolism. These miRNAs reduced the uptake of glucose and glutamine and prevented lactate build-up in the imatinib-resistant cells. Furthermore, the FBA analysis reveals the key metabolic reactions that can be targeted to overcome imatinib resistance.

Acknowledgement

The authors acknowledge the support received from the Central University of Punjab, Bathinda, in writing this manuscript. The authors are also gratified

to the Department of Science and Technology, New Delhi (DST-FIST- SR/FST/LS-I/2018/125©) for financial support under the DST-FIST programs to the Department of Biochemistry, Central University of Punjab. PS and VA are grateful to the CSIR, New Delhi, to award their fellowships.

Conflict of interest

All authors declare no conflict of interest.

References

1 Lim H, Poleksic A & Xie L, Exploring landscape of drug-target-pathway-side effect associations. *AMIA Jt Summits Transl Sci Proc*, 2018 (2018) 132.

2 Soverini S, Mancini M, Bavaro L, Cavo M & Martinelli G, Chronic myeloid leukemia: the paradigm of targeting oncogenic tyrosine kinase signaling and counteracting resistance for successful cancer therapy. *Mol cancer*, 17 (2018) 1.

3 Kumar V, Singh P, Gupta, SK, Ali V & Verma M, Transport and metabolism of tyrosine kinase inhibitors associated with chronic myeloid leukemia therapy: A review. *Mol Cell Biochem*, 477 (2022) 1.

4 Fava C, Rege-Cambrin G & Saglio G, Imatinib: the first-line CML therapy. In *Chronic Myeloid Leukemia*. *Springer Cham*, (2021), 49.

5 Buchdunge E, Cioffi CL, Law N, Stover D, Ohno-Jones S, Druker BJ, &Lydon NB, Abl Protein-Tyrosine Kinase Inhibitor STI571 Inhibits *In vitro* Signal Transduction Mediated by c-Kit and Platelet-Derived Growth Factor Receptors. *J Pharmacol Exp Ther*, 295 (2000) 139.

6 Ma L, Shan Y, Bai R, Xue L, Eide CA, Ou J, Zhu LJ, Hutchinson L, Cerny J, Khoury HJ & Sheng Z, A therapeutically targetable mechanism of BCR-ABL–independent imatinib resistance in chronic myeloid leukemia. *Sci Transl Med*, 6 (2014) 252.

7 Srivastava S, & Pandey A, Computational screening of anticancer drugs targeting miRNA155 synthesis in breast cancer. *Indian J Biochem Biophys*, 57(2020) 389.

8 Wang JX, Choi SY, Niu X, Kang N, Xue H, Killam J & Wang Y, Lactic Acid and an Acidic Tumor Microenvironment suppress Anticancer Immunity. *Int J Mol Sci*, 21 (2020) 8363.

9 DeBerardinis RJ, Lum JJ, Hatzivassiliou G & Thompson CB, The Biology of Cancer: Metabolic Reprogramming Fuels Cell Growth and Proliferation. *Cell Metab*, 7 (2008) 11.

10 Kominsky DJ, Klawitter J, Brown JL, Boros LG, Melo JV, Eckhardt SG & Serkova NJ. Abnormalities in Glucose Uptake and Metabolism in Imatinib-Resistant Human BCR-ABL–Positive Cells. *Clin Cancer Res*, 15 (2009) 3442.

11 Barnes K, McIntosh E, Whetton AD, Daley GQ, Bentley J & Baldwin SA. Chronic myeloid leukaemia: an investigation into the role of Bcr-Abl-induced abnormalities in glucose transport regulation. *Oncogene*, 24 (2005) 3257.

12 Lane AN & Fan TW, Regulation of mammalian nucleotide metabolism and biosynthesis. *Nucleic Acids Res*, 43 (2015) 2466.

13 Stephanopoulos G & Stafford DE, Metabolic engineering: a new frontier of chemical reaction engineering. *Chem Eng Sci*, 57 (2002) 2595.

14 Wuxiao Z, Wang H, Su Q, Zhou H, Hu M, Tao S, Xu L, Chen Y & Hao X, MicroRNA-145 promotes the apoptosis of leukemic stem cells and enhances drug-resistant K562/ADM cell sensitivity to adriamycin *via* the regulation of ABCE1. *Int J Mol Med*, 46 (2020) 1289.

15 He J, Han Z, An Z, Li Y, Xie X, Zhou J, He S, Lv Y, He M, Qu H & Liu G, The miR-203a Regulatory Network Affects the Proliferation of Chronic Myeloid Leukemia K562 Cells. *Front Cell Dev Biol*, 9 (2021) 616711.

16 Yang J, Yin Z, Li Y, Liu Y, Huang G, Gu C & Fei J, The Identification of Long Non-coding RNA H19 Target and Its Function in Chronic Myeloid Leukemia. *Mol Ther Nucleic Acids*, 19 (2020) 1368.

17 Karimiani EG, Marriage F, Merritt AJ, Burthem J, Byers RJ & Day PJR, Single-cell analysis of K562 cells: An imatinib-resistant subpopulation is adherent and has upregulated expression of BCR-ABL mRNA and protein. *Exp Hematol*, 42 (2014) 183.

18 Gupta SK, Singh P, Chhabra R & Verma M, Novel pharmacological approach for the prevention of multidrug resistance (MDR) in a human leukemia cell line. *Leuk Res*, 109 (2021) 106641.

19 Liu H, & Zhang Y, Effects of miR-222 on cisplatin resistance of renal cancer cell strains and related mechanisms. *Indian J Biochem Biophys*, 57(2020) 382.

20 WangF, Wang K, Tang M, WangQ, & Wei X, MicroRNA-9-5p inhibits osteosarcoma cell promotion, metastasis and resistance to apoptosis via negatively targeting Grb2-associated binding protein 2. *Indian J Biochem Biophys*, 57 (2020) 521.

21 Zhang M, Xiao F, Li Y, Chen Z, Zhang X, Xing W, Yuan W & Zhou Y, MiR-106b-25 promotes chemoresistance in acute myeloid leukemia *via* abolishing multiple apoptotic pathways. *Blood*, 138(2021) 4341.

22 Liao H, Bai Y, Qiu S, Zheng L, Huang L, Liu T, Wang X, Liu Y, Xu N, Yan X & Guo H, MiR-203 downregulation is responsible for chemoresistance in human glioblastoma by promoting epithelial-mesenchymal transition *via* SNAI2. *Oncotarget*, 6 (2015) 8914.

23 Li Y, Yuan Y, Tao K, Wang X, Xiao Q, Huang Z, Zhong L, Cao W, Wen J & Feng W, Inhibition of BCR/ABL Protein Expression by miR-203 Sensitizes for Imatinib Mesylate. *PLoS One*, 8 (2013) e61858.

24 Lu YH & Huang ZY, Global identification of circular RNAs in imatinib (IM) resistance of chronic myeloid leukemia (CML) by modulating signaling pathways of circ_0080145/miR-203/ABL1 and circ 0051886/miR-637/ ABL1. *Mol Med*, 27 (2021) 1.

25 Ferreira AF, Moura LG, Tojal I, Ambrósio L, Pinto-Simões B, Hamerschlak N, Calin GA, Ivan C, Covas DT, Kashima S & Castro FA, ApoptomiRs expression modulated by BCR–ABL is linked to CML progression and imatinib resistance. *Blood Cells Mol Dis*, 53 (2014) 47.

26 Chen X, Chen Y, Zhang M, Cheng H, Mai H, Yi M, Xu H, Yuan X, Liu S & Wen F, HucMSC exosomes promoted imatinib-induced apoptosis in K562-R cells *via* a miR-145a-5p/USP6/GLS1 axis. *Cell Death Dis*, 13 (2022) 1.

27 Kallifatidis G, Smith DK, Morera DS, Gao J, Hennig MJ, Hoy JJ, Pearce RF, Dabke IR, Li J, Merseburger AS & Kuczyk MA, β-arrestins regulate stem cell-like phenotype and response to chemotherapy in bladder cancer. *Mol Cancer Ther*, 18 (2019) 801.

28 Aslibekyan S, Brown EE, Reynolds RJ, Redden DT, Morgan S, Baggott JE, Sha J, Moreland LW, O'Dell JR, Curtis JR & Mikuls TR, Genetic variants associated with methotrexate efficacy and toxicity in early rheumatoid arthritis: results from the treatment of early aggressive rheumatoid arthritis trial. *Pharmacogenomics J*, 14 (2014) 48.

29 SouvickB, Elizabeth M, Madhumita R, & Sutapa M, (2020). PEITC by regulating Aurora Kinase A reverses chemoresistance in breast cancer cells. *Indian J Biochem Biophys*, 57 (2020) 167.

30 Gao YH, Wu ZX, Xie LQ, Li CX, Mao YQ, Duan YT, Han B, Han SF, Yu Y, Lu HJ & Yang PY, VHL deficiency augments anthracycline sensitivity of clear cell renal cell carcinomas by down-regulating ALDH2. *Nat Commun*, 8 (2017) 1.

31 Mostazo MG, Kurrle N, Casado M, Fuhrmann D, Alshamleh I, Häupl B, Martín-Sanz P, Brüne B, Serve H, Schwalbe H & Schnütgen F, Metabolic plasticity is an essential requirement of acquired tyrosine kinase inhibitor resistance in chronic myeloid leukemia. *Cancers*, 12 (2020) 3443.

32 Li J, Gu D, Lee SS, Song B, Bandyopadhyay S, Chen S, Konieczny SF, Ratliff TL, Liu X, Xie J & Cheng JX, Abrogating cholesterol esterification suppresses growth and metastasis of pancreatic cancer. *Oncogene*, 35 (2016) 6378.

33 Kotrikadze N, Alibegashvili M, Ramishvili L, Mikaia N, Khazaradze A, Sepiashvili B, Nakashidze I, Gordeziani M & Ahmad S, The role of lipids and fatty acid metabolism in the development of prostate cancer. *Indian J Biochem Biophys*, 59 (2022) 873.

34 Fan J, Lin R, Xia S, Boggon TJ, Curran WJ & Chen J, Tetrameric Acetyl-CoA Acetyltransferase 1 is important for tumor growth. *Mol Cell*, 64 (2016) 859.